

Path-Tree Optimization in Partially Observable Environments using Rapidly-Exploring Belief-Space Graphs

Camille Phipuepal¹, Andreas Orthey², Nicolas Viennot³ and Marc Toussaint²

Abstract—Robots often need to solve path planning problems where essential and discrete aspects of the environment are partially observable. This introduces a multi-modality, where the robot must be able to observe and infer the state of its environment. To tackle this problem, we introduce the Path-Tree Optimization (PTO) algorithm which plans a *path-tree* in belief-space. A path-tree is a tree-like motion with branching points where the robot receives an observation leading to a belief-state update. The robot takes different branches depending on the observation received. The algorithm has three main steps. First, a rapidly-exploring random graph (RRG) on the state space is grown. Second, the RRG is expanded to a belief-space graph by querying the observation model. In a third step, dynamic programming is performed on the belief-space graph to extract a path-tree. The resulting path-tree combines exploration with exploitation i.e. it balances the need for gaining knowledge about the environment with the need for reaching the goal. We demonstrate the algorithm capabilities on navigation and mobile manipulation tasks, and show its advantage over a baseline using a task and motion planning approach (TAMP) both in terms of optimality and runtime.

I. INTRODUCTION

Motion planning problems often assume that the environment is fully observable. However, in realistic scenarios, a robot will only have limited access to the environment through its sensors and can therefore only partially observe the state of the world. An example would be a robot, which has a blueprint of a building, but without knowing which doors are open or close. Another example would be a robot in a warehouse, where it has to get a package, but does not know in which location the package resides. In such environments, the robot has a countable number of hypotheses about the environment, which it can observe only in close proximity to certain objects. We say that such environments are partially observable and *multi-modal*.

Multi-modal environments require novel, more general approaches to planning. First, this requires a plan, which takes all possible outcomes into account, such that we have *contingencies* to control the robot irrespective of what observations were made. If a door is closed, the robot should know how to proceed. Second, this requires *optimal motions*, which minimize the expected cost to solve the problem at hand—not only contingencies, but optimal behavior over all modes.

Those requirements are difficult to model with existing frameworks based on task and motion planning (TAMP) or

optimization-based methods. Instead, we develop an integrated solution based on belief-space planning, which we call path-tree optimization (PTO). PTO extends previous research work [1], [2] which introduce tree-like motions computed with optimization based-methods in the respective sub-fields of Task and Motion Planning (TAMP) and Model Predictive Control (MPC). The concept of tree-like motions is extended here to sampling-based path planning, and leverages the strong guarantees of asymptotic optimality to tackle problems challenging for pure optimization-based methods (e.g. due to a high number of local minima). In addition, unlike [1], in which the observation actions are planned at the task level, the presented approach incorporates the observation model and the belief-state inference on the motion planning level directly, leading to a unified algorithm. Accordingly, the main contributions of the paper are:

- a general sampling-based algorithm planning optimal path-trees for partially observable multi-modal problems.
- the demonstration of the applicability of the method on low-dimensional navigation tasks, as well as on high-dimensional mobile manipulation problems.

II. RELATED WORK

Path planning under partial observability and multi-modality of the environment state is related to the broader topic of path-planning under uncertainty for which many adaptations of classical sampling-based planners [3], [4] have been developed.

One group of algorithms aims to tackle the localization uncertainty by planning paths which not only reach a goal but also minimize the localization uncertainty [5] [6]. Like the presented approach, those algorithms plan in belief-space on a graph grown in a sampling-based fashion. An observation model is used to infer the belief-state dynamic. However, those algorithms model partial observability over continuous variables (the localization), and assume gaussian belief-states, while we plan over discrete variables and plan reactive path-trees for different possible observations.

Another closely related line of work plans paths which maximize the information gathered along the path [7] [8] [9]. Like the previously mentioned work, a graph or tree is grown in a sampling-based fashion. However, instead of planning in belief-space, those approaches determine the optimal traversal w.r.t. an information objective, e.g. volumetric gain for the use case of mapping in [9].

Another direction of research uses sampling-based methods for planning problems where the goal is expressed as a temporal logic specification [10] [11] [12]. Similarly to

¹Machine Learning & Robotic Lab, University of Stuttgart, Germany
camille.phiquepal@ipvs.uni-stuttgart.de

²Learning and Intelligent Systems Lab, TU Berlin, Germany
toussaint@tu-berlin.de

³nicolas.viennot@cs.columbia.edu

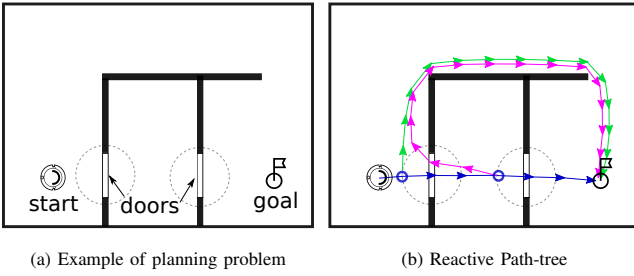


Fig. 1: The robot has to reach the goal region. The doors state (open vs. closed) is only observable in their vicinity. PTO plans path-trees with observation points (blue circles) and path-contingencies (blue, green, magenta) reacting to the observations.

the method of this paper, the output solution of the planning problem is more general than a sequence of states. In [10] [12], the solutions are cyclic infinite paths. The closest to our proposed approach is [11]. It synthesizes control policies in belief-space that react to observations. The goal is specified using GDTL (Gaussian Distribution Temporal Logic). Like the other belief-space planning approaches previously mentioned ([5] [6]), the considered uncertainty is over the robot localization, and belief-states are modeled as gaussians. In contrast, the presented approach focuses on the environment uncertainty, it does not assume gaussian beliefs but describes the environment uncertainty as a finite and countable set of hypotheses.

In the field of object manipulation planning [13] also presents similarities to our approach. It finds contingency plans based on contact sensing. Contacts help to reduce the uncertainty over the relative position of the object to manipulate. It is a continuous uncertainty, while this paper focuses on the environment multi-modality. In addition, we aim for optimality whereas [13] aims only for feasible policies.

III. PROBLEM FORMULATION

We optimize policies in a context of mixed-observability. The robot state is fully observable, but discrete and essential parts of the environment are only partially observable. In the example of the Fig. 1a this models the fact that each door can be open or closed.

To capture this mixed observability structure, we adopt a compound state representation where a state is composed of 2 parts:

- $x \in \mathbb{R}^n$ is a continuous state and corresponds to the usual notion of state in the path planning literature.
- $s \in \mathcal{H}$ is a discrete state from a finite set of world hypotheses \mathcal{H} .

In the problem introduced in Fig. 1a the variable s can take four possible values corresponding to the possible states of the environment as illustrated on Fig. 2.

The robot is not oblivious about the likelihood of each state hypothesis. On the problem introduced on Fig. 1a, when the robot is in the vicinity of a door (symbolized with the circles), it receives an observation indicating whether the door is open or not.



Fig. 2: Partially observable discrete state: With 2 partially observable doors, there are 4 possible states of the environment.

Planning is performed in belief-space, where a belief-state b is a probability distribution over the possible states.

A. Path-tree

The algorithm consists in planning a path-tree. A path-tree is a single path, which branches into multiple possible paths at designated observations states where the belief-states change. As schematically shown on Fig. 1b, the path-tree starts from a single root node and finishes with leaf nodes satisfying the goal condition. The path-tree branches where the robot receives an observation leading to a belief-state update. The different branches of the path-tree are the different planned contingencies. To be complete, a path-tree must end inside the goal region for all $s \in \mathcal{H}$.

In addition, we assume the observation model to be binary, meaning that $p(s|o) \in \{0.0, 1.0\}, \forall s \in \mathcal{H}, \forall o \in O$, where o is an observation from the observation space O . This property is important. It guarantees that the number of belief-states is finite and can be enumerated which is needed for the graph expansion to belief-state presented in IV-C. For the example of Fig. 1a, it means that observations indicate whether the door is open or not without uncertainty. In addition, it typically implies that the number of branchings N_o stays small compared to the total number of states N on the path-tree. In other words $N_o \ll N$. It can be understood easily on the presented example: once an observation has been received for a door, the agent knows with certainty if the door is open or not, such that the next observations of the same door do not lead to an update of the belief-state.

B. Optimization objective

We note ψ a path tree, and (u, v) consecutive nodes on the tree ψ . The motion cost between two nodes u and v is given by a cost function $C(u, v)$. In addition, we note $p(u|\psi, b_0)$ the probability to reach a node u . This probability depends on the initial belief-state b_0 and the observation model.

In the presence of uncertainty we minimize the expectation of the motion costs, such that the partially observable multi-modal optimization problem is defined as follows.

$$\psi^* = \operatorname{argmin}_{\psi} \sum_{(u,v) \in \psi} C(u, v) p(v|\psi, b_0), \quad (1a)$$

s.t.

$$\forall s \in \mathcal{H} \exists l \in \mathcal{L}(\psi) \mid G(l), \quad (1b)$$

$$\mathcal{V}(u, v), \forall (u, v) \in \psi, \quad (1c)$$

$$b_v(s) = p(s|o) \times b_u(s), \forall s \in \mathcal{H}, \forall (u, o, v) \in \psi, \quad (1d)$$

where the $\mathcal{L}(\psi)$ gives the leaf nodes of ψ , and $G(l)$ is the goal predicate, indicating whether a node fulfills the goal conditions. Eq. (1b) states that ψ shall be complete i.e. there

is a leaf node satisfying the goal conditions for each possible s .

Eq. (1c) expresses that ψ shall be composed of feasible motions (e.g. collision free, feasible given the robot motion model), and $\mathcal{V}(u, v)$ is the predicate encoding the validity of the transition between u and v .

Finally, Eq. (1d) corresponds to the bayesian updates according to the observation model. The symbol o is the observation received when transitioning from u to v . The belief-state of the node v is noted b_v , and $p(s|o)$ is the observation model.

It is noteworthy, that the problem formulation doesn't contain any term explicitly inciting the robot to explore its environment. The balance exploration / exploitation emerges naturally as a result of the minimization of the expected motion costs.

IV. PATH-TREE OPTIMIZATION (PTO)

To build a path-tree satisfying the specification of Equation 1, we proceed stepwise. First a transition system is grown in a sampling based fashion until the existence of a solution is guaranteed. This corresponds to the two first steps schematized on Fig. 3. In a second step, the optimal path-tree is extracted using dynamic programming.

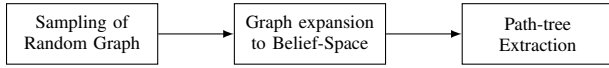


Fig. 3: PTO Algorithm overview. It contains three main steps corresponding to the algorithms described in the sections IV-B, IV-C and IV-D.

A. Interface between the algorithm and the application layer

The connection between the core of the algorithm and a given planning problem is achieved via 4 functions that the application layer provides:

- **STATECHECK**, which takes a robot configuration x as input and returns the list of worlds in which the configuration is valid.
- **TRANSITIONCHECK**, which takes two robot configurations as inputs and returns the list of worlds in which the robot configurations is valid.
- **GOALCHECK**, which takes a robot configuration as input and returns the list of worlds in which the robot configuration fulfills the goal conditions.
- **OBSERVE**, which receives a robot configuration and a belief-state as inputs and returns the possible output belief-states.

The functions **STATECHECK**, **TRANSITIONCHECK** and **GOALCHECK** are akin to the functions required by standard path-planners like OMPL [14], but they are more general: the return type is a list of worlds instead of a boolean.

The **OBSERVE** function is directly linked to partial observability and is specific to this algorithm. It allows belief-state inference. Going back to the example of Fig. 1a, **OBSERVE** returns an unchanged belief-state for all robot configurations that are outside of the door visibility zone, this is because no observation can be received, and therefore no belief-state

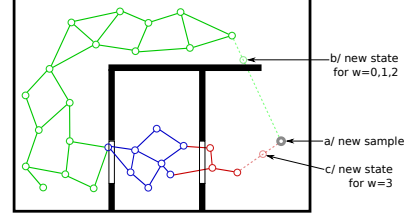


Fig. 4: Random Graph expansion: For a new sample a), the new state is computed steering from the closest compatible node of the graph. The closest compatible node depends on the sample world w , see a) and c).

inference is done. On the other hand, up to two possible belief-states are returned for robot configurations inside the door visibility zone. They correspond to the updated belief-states for the two possible observations.

The following sections detail how the calls to those functions are orchestrated by the algorithm to build a path-tree.

B. Rapidly-exploring Random Graph

In this first step, a random-graph is grown in a sampling based fashion. To avoid the curse of dimensionality, sampling is not performed in belief-space directly but in the robot configuration space. The random graph is an intermediate representation and will be expanded to belief-state in a second step as described in the next section.

The nodes of the random graph are associated with:

- a robot configuration x , which is randomly sampled.
- a list worlds \mathcal{F} in which the robot configuration is fulfilling the goal condition. This is obtained by querying the function **GOALCHECK**.

The edges of the random graph are associated with:

- a list of worlds \mathcal{W} in which the transition is valid. This is obtained by calling the function **TRANSITIONCHECK**.

The random-graph creation is described in Alg. 1. First, the state is sampled (lines 4). Then the new state is steered from a neighbor node of the graph (line 7). Unlike RRT where the new state is steered from the nearest neighbor, here, the selected neighbor is the nearest neighbor having world validities \mathcal{W} containing the sampled world w (line 5), as illustrated on Fig. 4. This additional condition for the neighbor selection is to ensure that the random graph contains paths to the goal for each world.

If the new state is valid for at least one world (line 9), the goal conditions are checked (line 10) and a new node is added to the random-graph (line 11). Finally, the new node is connected to neighboring nodes (lines 13 to 16), which are all nodes in an adaptive radius [15] having world validities containing w .

This procedure is repeated until the graph is complete meaning that it will allow the successful extraction of a solution path-tree (see line 3). To implement the function **ISCOMPLETE** we assume in our examples that the transitions are *symmetrical*, i.e. if a motion exists from a node u to v , then a motion between v and u also exists. Under this assumption, the random-graph contains a solution path-tree

as soon as the set of leaf nodes is complete, in the sense that it covers every possible world, i.e. $\bigcup_{u \in \mathcal{L}(\mathcal{G})} \mathcal{F}_u = \mathcal{H}$. Indeed, the fact that the set of leaf nodes is complete implies that for each possible world, a path from the root to a leaf exists. A naive solution is therefore to execute those paths in sequence, and potentially *backtrack* to the root node if a path doesn't reach the goal (hence the required assumption regarding the symmetrical transition). In practice, once the completeness threshold is reached, a solution can be extracted which is typically more optimal than the aforementioned worst-case backtracking strategy. Our implementation also has a minimum number of iterations, to further expand the random-graph even beyond the completeness threshold to improve the quality of the path-trees.

Algorithm 1 Rapidly-exploring Random Graph

```

1: function BUILDRRG( $q_{start}$ )
2:    $\mathcal{G} \leftarrow \text{INIT}(\mathcal{G}, q_{start})$ 
3:   while  $\neg \text{ISCOMPLETE}(\mathcal{G})$  do
4:      $q_{rand} \leftarrow \text{SAMPLESTATE}()$ 
5:      $w \leftarrow \text{SAMPLEWORLD}()$ 
6:      $q_{near} \leftarrow \text{NEAREST}(q_{rand}, w)$ 
7:      $q_{new} \leftarrow \text{STEER}(q_{near}, q_{rand})$ 
8:     /*get relevant info of the new state and add it to the graph*/
9:     if  $\text{STATECHECK}(q_{new}) \neq \emptyset$  then
10:       $\mathcal{F} \leftarrow \text{GOALCHECK}(q_{new})$ 
11:       $\mathcal{G} \leftarrow \text{ADDNODE}(q_{new}, \mathcal{F})$ 
12:      /*get relevant edges info and add them to the graph*/
13:      for  $q_{near} \in \text{NEARESTS}(q_{new}, w)$  do
14:         $\mathcal{W} \leftarrow \text{TRANSITIONCHECK}(q_{near}, q_{new})$ 
15:        if  $\mathcal{W} \neq \emptyset$  then
16:           $\mathcal{G} \leftarrow \text{ADDEDGE}(q_{near}, q_{new}, \mathcal{W})$ 

```

C. Graph expansion to belief-space

At this stage, a random-graph \mathcal{G} has been built, and the existence of a path-tree solution is guaranteed, however, the random-graph is still an intermediate representation that cannot be used directly to optimize path-trees. In this step, a transition system in belief-space, or belief-graph \mathcal{B} is constructed out of \mathcal{G} by querying the observation model. The nodes of the belief-graph are associated with:

- a robot-configuration x .
- a belief-state b .

The edges of the belief-graph are associated with:

- the observation o making the transition between the beliefs on the incoming and out-coming nodes.

The belief-graph can be understood as the random-graph replicated over several layers, where each layer is a different belief-state, as shown on Fig. 5. The transitions within one layer correspond to robot motions, whereas the transitions from one layer to another correspond to the integration of an observation leading to a belief-state update. The motion transitions are, in general, not identical across belief-states.

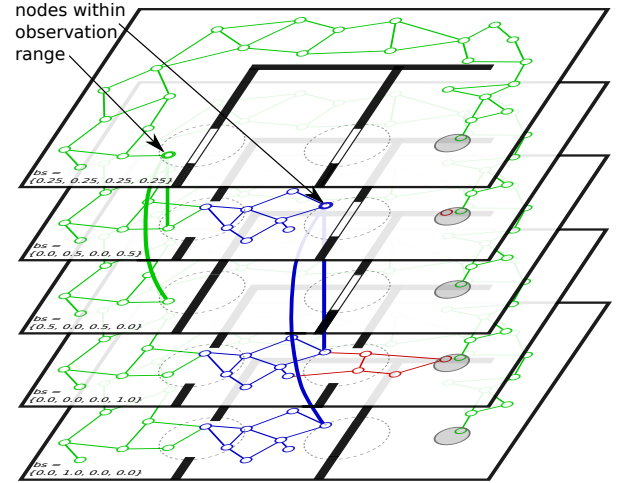


Fig. 5: Random Graph expanded to belief-state: The belief-states are represented as *layers* of the belief-graph. The nodes within the observation range potentially lead to a belief-state update and therefore have edges transitioning to other belief-states (thick vertical edges).

For example, on Fig. 5, the transitions crossing through the doors exist only in beliefs compatible with an open door.

The construction procedure is given by the Alg. 2. First, the edges of \mathcal{G} are replicated to the belief-states compatible with the edge's valid worlds (line 3 to 7).

Second, the observation model is called via the function OBSERVE to identify where edges should be created between belief-states (lines 9 to 12). The belief-state-transition edges due to observations are represented by vertical lines going from one layer to another on Fig. 5.

Algorithm 2 Creation of the belief-graph

```

1: function BUILDBELIEFGRAPH( $b_{start}, \mathcal{G}$ )
2:   /*connect nodes within the same belief*/
3:   for  $e \in \mathcal{G} \text{ edges}$  do
4:     for  $b \in \text{BELIEFS}(e \text{ world\_validities})$  do
5:        $u \leftarrow \mathcal{B} \text{ ADDNODE}(b, e \text{ from})$ 
6:        $v \leftarrow \mathcal{B} \text{ ADDNODE}(b, e \text{ to})$ 
7:        $\mathcal{B} \leftarrow \text{ADDEDGE}(u, v)$ 
8:   /*create transitions between beliefs due to observations*/
9:   for  $u \in \mathcal{B} \text{ nodes}$  do
10:     $V \leftarrow \text{OBSERVE}(u)$ 
11:    for  $v \in V$  do
12:       $\mathcal{B} \leftarrow \text{ADDEDGE}(u, v)$ 

```

The belief-graph \mathcal{B} is significantly larger than the random graph \mathcal{G} since there are multiple belief-states corresponding to one same robot configuration. However, its construction only calls the observation model (function OBSERVE). In contrast, the random-graph is smaller but its creation calls the collision checks (STATECHECK and TRANSITIONCHECK) in addition to the nearest neighbor search that are expensive.

D. Policy extraction

At this stage, the belief-graph \mathcal{B} is fully built, and it contains at least one path-tree satisfying the goal conditions

(Eq. 1b). The goal is now to find the optimal path-tree by minimizing the expected costs to goal (Eq. 1a).

The expected costs to goal are computed for each node of \mathcal{B} . This is done using dynamic programming and by iteratively applying Bellman updates on each node of \mathcal{B} . The procedure is described by the Algorithm 3.

The algorithm is similar to the Dijkstra algorithm [16] in the way the nodes are prioritized using a priority queue (lines 2 to 13). For edges corresponding to a robot motion, the Bellman update is also the same as in Dijkstra (lines 15 and 16). However, for edges corresponding to an observation, the Bellman update of the parent node differs and is the sum of the children's expected costs weighted by their respective branching probabilities (lines 17 to 19).

Algorithm 3 Computation of the expected costs to goal

```

1: function COMPUTEEXPECTEDCOSTTOGOAL( $\mathcal{B}$ )
2:    $Q \leftarrow \text{PRIORITYQUEUE}()$ 
3:   /*Initialization*/
4:   for  $n \in \mathcal{B}.\text{nodes}$  do
5:     if ISFINAL( $n$ ) then
6:        $C[n] \leftarrow 0.0$ 
7:        $Q.\text{PUSH}(n, 0.0)$ 
8:     else
9:        $C[n] \leftarrow +\infty$ 
10:  /*The main loop*/
11:  while  $\neg \text{ISEMPTY}(Q)$  do
12:     $v \leftarrow \text{POP}(Q)$ 
13:    for  $u \in \text{PARENTS}(v)$  do
14:      /*Bellman update dependent on the edge type*/
15:      if ISACTIONEDGE( $u, v$ ) then
16:         $c \leftarrow \text{COST}(u) + C[v]$ 
17:      else if ISOBSERVATIONEDGE( $u, v$ ) then
18:         $\mathcal{W} \leftarrow \text{OBSERVATIONCHILDREN}(u)$ 
19:         $c \leftarrow \sum_{\nu \in \mathcal{W}} p(\nu|u) \times C[\nu]$ 
20:      if  $c < C[u]$  then
21:         $C[u] \leftarrow c$ 
22:         $Q.\text{PUSH}(u, c)$ 

```

Once the expected costs to goal are known for each node, the optimal path-tree can be built straightforwardly starting from the root and recursively appending the best next child, or next best children (in case of a node with an observation branching).

Optimizing w.r.t. the expected costs to goal naturally results in an exploration vs. exploitation trade-off, i.e. path-trees balance the need for moving towards configurations providing informative observations vs. the need to advance towards the goal.

E. Path-tree refinement

At this stage, a solution path-tree has already been extracted. However, despite asymptotic optimality guarantee, a path-tree may contain unnatural or jerky motions due to the random nature of the random-graph creation. While we could increase the number of iterations, this would become

costly in terms of runtime. To tackle this phenomenon, we add a refinement step, working piecewise: the path-pieces between observation branchings are refined independently using the partial-shortcut method [17]. The branching nodes corresponding to observations are extremities of the path pieces and they form the junctions between path pieces. Those nodes are not modified by the refinement procedure.

F. Completeness and optimality

We argue that PTO is probabilistically complete and asymptotically optimal, i.e. it will eventually solve Eq. (1) to the optimal solution. Our reasoning is divided into two steps. First, since we use an asymptotically optimal sampling-method [18], [15] on every modality (Alg. 1), together with a uniform modality sampler, PTO will eventually converge to the optimal solution on each mode. Second, by inter-connecting edges between modalities, we guarantee that we account for possible mode-changes which can only happen in observation nodes (Alg. 2). The final belief-graph will therefore contain the optimal solution, which we can then extract using the Dijkstra-like algorithm in our policy extraction step (Alg. 3). This combination guarantees that the optimal solution will eventually be attained in the limit.

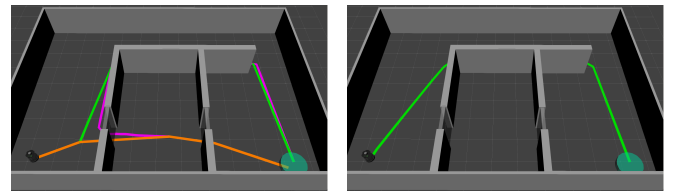
V. EXPERIMENTS

The path-tree optimization algorithm is implemented in the Rust programming language [19]. The application layer is implemented in C++ using MoveIt [20]. The source code and a supplementary video are available for reference ¹.

A. Mobile robot navigation

We consider two planning problems similar to the initial example introduced in Fig. 1. The robot is the Kobuki platform. The robot has to reach a predefined goal region, but it doesn't know at planning time, which doors are open. The observation model simulates that the sensor mounted on the Kobuki and the perception pipeline allow the robot to know if a door is open once the robot is close to a door (less than 1.5 m) and has a non-occluded line of sight to the door. We plan for the two-dimensional position of the robot.

The first problem, called problem-A (Fig. 6) has two uncertain doors. The second problem, called problem-B (Fig. 8) is more complex, the map is larger, there are four doors, and more obstacles.



(a) Path-tree obtained with a high likelihood that doors are open (80%). The path-tree has 2 branching points corresponding to the observation of the 2 doors.

(b) Path-tree obtained with 50% of likelihood that doors are open: It is not advantageous to attempt the direct way through the doors.

Fig. 6: Problem-A: The robot has to reach the green region on the right.

¹<https://github.com/cambyse/po-rrt>

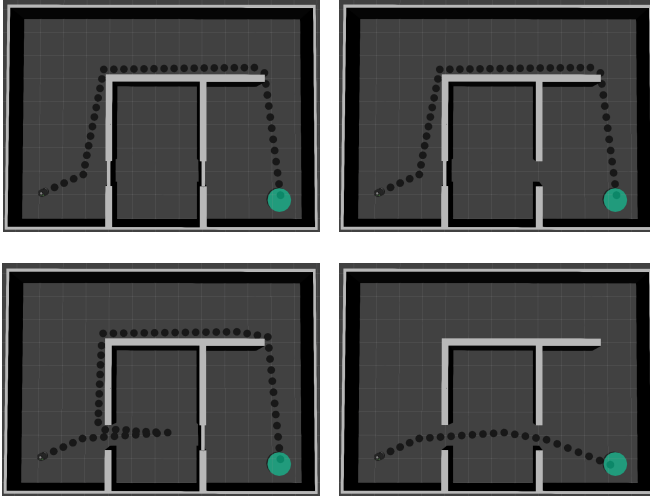


Fig. 7: Path-tree execution in several worlds: The robot potentially has to backtrack if it ends up in a dead-end after observing the second door.

Fig. 6a shows the path-tree obtained when the initial belief-state corresponds to a high likelihood that each door is opened (80%). In that case, it is advantageous to attempt the direct path through the doors. The path-tree has two branching points corresponding to the observations of the two doors. Fig. 7 shows the execution of the path-tree in each possible world. In the best case, the two doors are open and the robot reaches the goal directly. In the worst-case, the robot ends up in a dead-end and has to backtrack after observing that the second door is closed.

In this example, we see the strong influence of the initial belief-state on the topology of the path-tree: Fig. 6b shows the path-tree obtained with an initial belief-state corresponding to a probability of only 50% that the doors are open. In that case, it is not worthy to attempt the way through the doors, the planned path takes the longer, but sure way to the goal. The path-tree boils down to a sequential path without observing branching points.

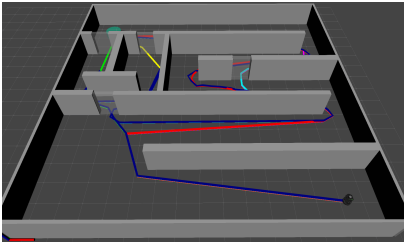


Fig. 8: Path-tree for Problem-B: The map has four doors leading to a more complex path-tree.

Fig. 8 shows the path-tree obtained for the problem-B, and Fig. 9 shows its execution in a subset of the possible worlds. The higher number of doors leads to a path-tree which is much more complex.

Table I, gives the expected costs to goal, and the planning times obtained when running the planning algorithm 20 times. Each problem is solved using 2 different strategies for the RRG sampling: In the initial variation, the RRG sampling is stopped as soon as completeness is guaranteed (see IV-B), and the second variations (A' and B') use a minimum number of 5000

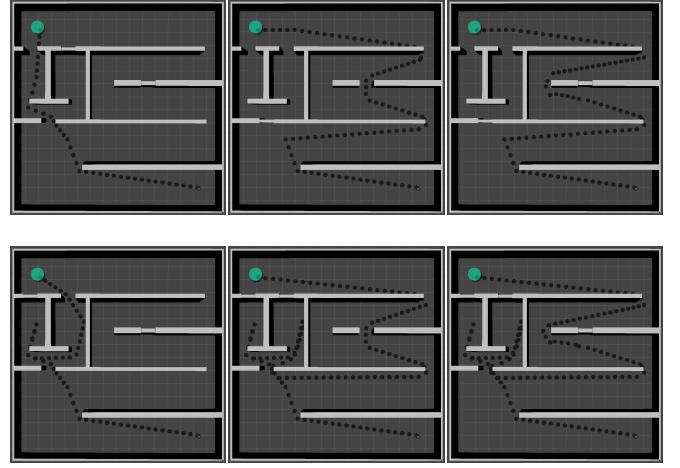


Fig. 9: Path-tree execution: The robot explores the doors on the left of the map. It potentially has to back-track and take the long route if it is blocked.

	# of iter	random graph creation	belief-space expansion	policy extraction	partial shortcut	path cost	total planning time (ms)
A	433 (107)	0.72 (0.44)	0.98 (0.51)	0.54 (0.27)	0.49 (0.28)	18.6 (0.37)	2.78 (1.4)
A'	5000 (0)	30.9 (3.7)	29.1 (2.80)	16.7 (1.1)	0.31 (0.05)	18.17 (0.1)	77.1 (6.02)
B	3956 (626)	44.7 (14.3)	345 (102)	173 (60.8)	3.25 (1.07)	45.1 (1.74)	567 (174)
B'	5000 (0)	61.5 (6.49)	538 (32)	270 (22.9)	2.95 (0.38)	43.9 (1.25)	873 (47.1)

TABLE I: Planning time and expected cost: The mean value is given first. The standard-deviation is in parentheses. Times are in milliseconds.

iterations to obtain a more qualitative path-tree.

Generally, the algorithm is fast, and takes less than 1 second even for the most complex map. The step taking the longest time is the graph expansion to belief-space (see IV-C). The reason is that the number of belief-states grows quickly when the number of doors increases, and the observation model is queried for each belief-space node.

Increasing the number of iterations results in smaller expected costs of the path-tree, at the expense of the overall runtime. In practice, the final refinement step (see IV-E) leads to path-trees that are already near-optimal even without a very high number of iterations, such that it is an efficient strategy to keep a small number of minimal iterations.

B. Robot arm object fetching

Our next scenario is a Panda arm robot mounted on a mobile base. We introduce two examples, where the task is to pick-up an object which is at an unknown location (see problem-A on Fig. 10 and problem-B on Fig. 11). The robot has prior knowledge of several potential locations, but the actual location is unknown at planning time.

The observation model simulates that a sensor is placed on the robot gripper and that the perception pipeline detects

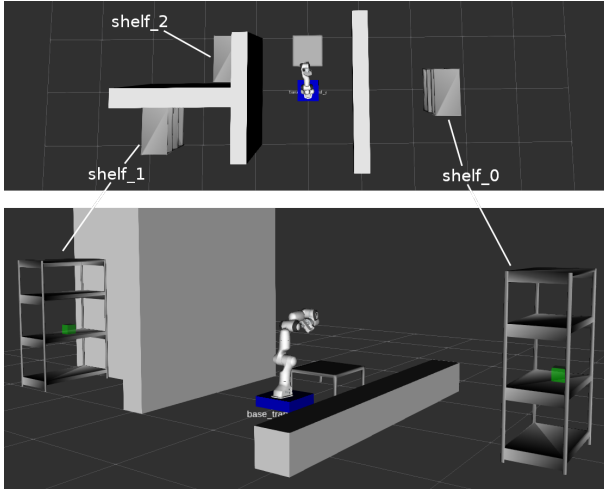


Fig. 10: Problem-A: The robot has to pick the green block. The block location is unknown, it may be on each one of the three shelves.

the block when it is within the sensor field of view (60°), at a distance less than 2 meters from the sensor, and not occluded by other objects (e.g. the walls).

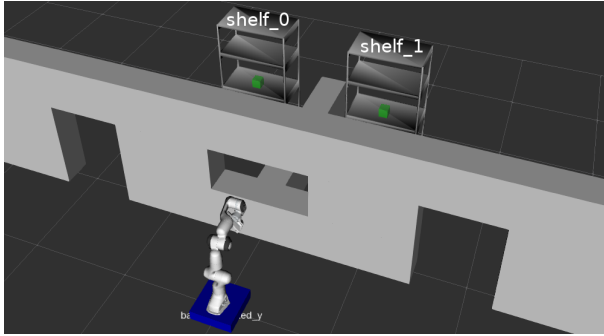


Fig. 11: Problem-B: The block might be on two different shelves. The opening between the two doors potentially allows the robot to observe the shelves without entering the rooms.

Planning is performed in joint space with 9 degrees of freedom (2 for the base, and 7 for the robot arm). Fig. 12 shows the trajectory of the robot base. There are two observation branching points corresponding to the observations of the two shelves. Fig. 13 shows the robot configuration at the

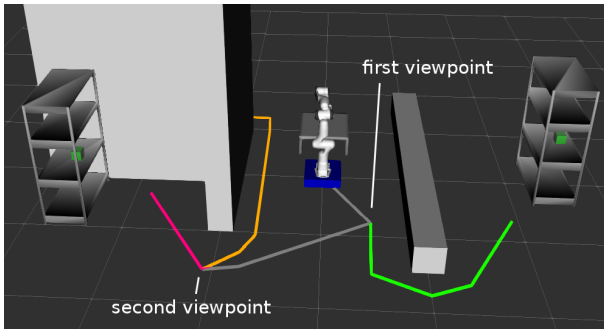


Fig. 12: Path-tree for Problem-A: The path tree first moves towards the shelf_0 to reach the first viewpoint. If the object is on the shelf_0, the green path is executed. Otherwise the robot moves towards the second viewpoint.

	# of iter	random graph creation	belief-space expansion	policy extraction	partial shortcut	path cost	total planning time (s)
A	10521 (16481)	5.86 (14.7)	0.31 (0.66)	0.30 (0.66)	0.43 (0.06)	3.27 (0.53)	6.75 (15.8)
B	4578 (3484)	1.28 (2.05)	0.03 (0.04)	0.01 (0.02)	0.26 (0.03)	3.72 (0.46)	1.59 (2.10)

TABLE II: Path-tree cost and planning time obtained over 100 planning queries: It indicates the mean value and the standard deviation in parentheses. Planning times are in seconds.

branching point of the path-tree. The opening in the wall allows the robot to take a look at the shelf.

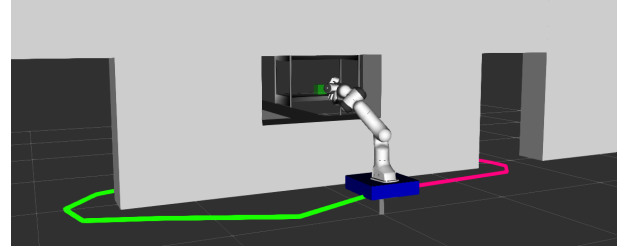


Fig. 13: Path-tree for Example-B: A first common branch of the path-tree leads the robot to an observation point through the opening. Depending on the observation, the robot will execute the green or the magenta path.

We report in Table II on the average path-tree cost and planning time obtained over 100 planning queries. In contrast to the examples of the previous section V-A, the planning time is dominated by the random graph creation. This is consistent with the fact that the geometric collision checks are more computationally expensive with this robot. In addition, we note that the planning times have a large dispersion around the mean value (see the standard deviation on II), which is due to the higher geometric complexity and dimensionality of the planning problem. Overall, the planning time remains limited to a few seconds.

C. Comparison to baseline

We compare PTO to a Task and Motion Planning (TAMP) approach, where the planning is hierarchical: it interleaves a symbolic search defining high level plans, and a motion planning phase computing the corresponding motions. The comparison is performed on variations of the shelf domain (Fig. 14a), where we plan for the 2D base position only. The number of shelves is varied to compare the scalability.

The high level search is performed using the Branch and Bound algorithm [21]. It explores the space of the possible sequences for visiting all the shelves. The nodes of the search correspond to shelves. The motion planner is queried when a node is created. For each node/shelf, 2 paths are planned using RRT*: the path to an observation point, and the path to fetch the object (to be executed if the object is actually detected). A path-tree is obtained by gathering the path pieces from the root node to a leaf of the search tree.

The branch and bound tree search is performed in a depth-first fashion, which leads to a quick first solution path-tree.

The best solution path-tree found so far is an upper bound of the cost and allows the pruning of a majority of the search tree. We report on Figure 14 on the average expected cost of the resulting path-trees, as well as on the planning times for each algorithmic step obtained by running PTO 100 times.

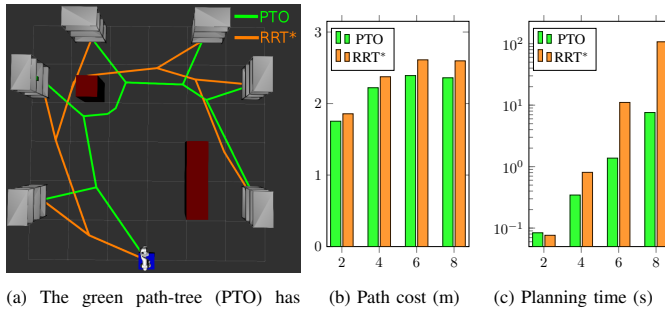


Fig. 14: Comparison of PTO to RRT*: 14b and 14c give the costs and planning times for different number of shelves. PTO provides path-trees with lower costs. Planning time (in log scale) also scales better.

First, we observe that PTO consistently leads to lower path-tree costs than the piece-wise planning with RRT*. This can be understood easily as the decomposition into piecewise motions leads to path pieces that are optimal w.r.t the sub-problem of reaching one shelf, but taken together, they don't form an optimal path-tree. On the other hand, PTO searches for a globally optimal path-tree. It is visible on Fig. 14a: the RRT* path-tree greedily moves towards the next shelf to explore, whereas PTO takes a less direct path to the observation point, which overall leads to a shorter path-tree.

Second, PTO scales better w.r.t. the number of shelves (see Fig. 14). Planning times are comparable for the variation with 2 shelves, but the difference between PTO and RRT becomes larger when the number of shelves increases. The main reason for this is that PTO is more sample-efficient: The random graph creation (see IV-B) which involves state and transition checks is constructed just once. On the other hand, the Branch and Bound + RRT* approach is more sample-intensive since a new random tree is re-sampled from scratch for the planning of each path-piece.

In this example, both algorithms PTO and the Branch and Bound search could be made faster by using heuristics as lower bound of the path costs (e.g. euclidean distance). We chose, however, to compare the general approaches, without optimizations tailored to the particular example.

VI. CONCLUSIONS

We proposed a new sampling-based path planning algorithm (PTO) for motion planning problems where discrete and critical aspects of the world are partially observable. The algorithm not only optimizes feasible motions but also plans observation points that allow the robot to gain knowledge about its environment to achieve its task. The resulting motions are path-trees in belief-space that react to observations. We argued that PTO is asymptotically optimal, and we showed that PTO compares advantageously to Task

and Motion Planning (TAMP) approaches both in terms of optimality and runtime efficiency.

REFERENCES

- [1] C. Phiquepal and M. Toussaint, "Combined Task and Motion Planning under Partial Observability: An Optimization-Based Approach," *IEEE International Conference on Robotics and Automation (ICRA)*, pp. 9000–9006, 2019.
- [2] C. Phiquepal and M. Toussaint, "Control-tree optimization: an approach to mpc under discrete partial observability," *IEEE International Conference on Robotics and Automation (ICRA)*, pp. 9666–9672, 2021.
- [3] S. M. LaValle *et al.*, "Rapidly-exploring random trees: A new tool for path planning," 1998.
- [4] L. E. Kavraki, P. Svestka, J.-C. Latombe, and M. H. Overmars, "Probabilistic roadmaps for path planning in high-dimensional configuration spaces," *IEEE transactions on Robotics and Automation*, vol. 12, no. 4, pp. 566–580, 1996.
- [5] S. Prentice and N. Roy, "The belief roadmap: Efficient planning in linear pomdps by factoring the covariance," in *Robotics research*, pp. 293–305, Springer, 2010.
- [6] A. Bry and N. Roy, "Rapidly-exploring random belief trees for motion planning under uncertainty," in *2011 IEEE international conference on robotics and automation*, pp. 723–730, IEEE, 2011.
- [7] G. A. Hollinger and G. S. Sukhatme, "Sampling-based robotic information gathering algorithms," *The International Journal of Robotics Research*, vol. 33, no. 9, pp. 1271–1287, 2014.
- [8] D. Levine, B. Luders, and J. How, "Information-rich path planning with general constraints using rapidly-exploring random trees," in *AIAA Infotech@ Aerospace 2010*, p. 3360, 2010.
- [9] T. Dang, M. Tranzatto, S. Khattak, F. Mascari, K. Alexis, and M. Hutter, "Graph-based subterranean exploration path planning using aerial and legged robots," *Journal of Field Robotics*, vol. 37, no. 8, pp. 1363–1388, 2020.
- [10] S. Karaman and E. Frazzoli, "Sampling-based motion planning with deterministic μ -calculus specifications," in *Proceedings of the 48th IEEE Conference on Decision and Control (CDC)*, pp. 2222–2229, IEEE, 2009.
- [11] K. Leahy, E. Cristofalo, C.-I. Vasile, A. Jones, E. Montijano, M. Schwager, and C. Belta, "Control in belief space with temporal logic specifications using vision-based localization," *The International Journal of Robotics Research*, vol. 38, no. 6, pp. 702–722, 2019.
- [12] C. I. Vasile, X. Li, and C. Belta, "Reactive sampling-based path planning with temporal logic specifications," *The International Journal of Robotics Research*, vol. 39, no. 8, pp. 1002–1028, 2020.
- [13] E. Páll, A. Sieverling, and O. Brock, "Contingent contact-based motion planning," in *2018 IEEE/RSJ International Conference on Intelligent Robots and Systems (IROS)*, pp. 6615–6621, IEEE, 2018.
- [14] I. A. Şucan, M. Moll, and L. E. Kavraki, "The Open Motion Planning Library," *IEEE Robotics & Automation Magazine*, vol. 19, pp. 72–82, December 2012. <https://ompl.kavrakilab.org>.
- [15] K. Solovey, L. Janson, E. Schmerling, E. Frazzoli, and M. Pavone, "Revisiting the asymptotic optimality of rrt," in *2020 IEEE International Conference on Robotics and Automation (ICRA)*, pp. 2189–2195, IEEE, 2020.
- [16] M. Sniedovich, "Dijkstra's algorithm revisited: the dynamic programming connexion," *Control and Cybernetics*, vol. 35, pp. 599–620, 2006.
- [17] R. Geraerts and M. H. Overmars, "Creating high-quality paths for motion planning," *The international journal of robotics research*, vol. 26, no. 8, pp. 845–863, 2007.
- [18] S. Karaman and E. Frazzoli, "Sampling-based algorithms for optimal motion planning," *The international journal of robotics research*, vol. 30, no. 7, pp. 846–894, 2011.
- [19] N. D. Matsakis and F. S. Klock II, "The rust language," in *ACM SIGAda Ada Letters*, vol. 34, pp. 103–104, ACM, 2014.
- [20] D. Coleman, I. Sucan, S. Chitta, and N. Correll, "Reducing the barrier to entry of complex robotic software: a moveit! case study," *arXiv preprint arXiv:1404.3785*, 2014.
- [21] D. R. Morrison, S. H. Jacobson, J. J. Sauppe, and E. C. Sewell, "Branch-and-bound algorithms: A survey of recent advances in searching, branching, and pruning," *Discrete Optimization*, vol. 19, pp. 79–102, 2016.